Controlled bioactive compound delivery systems based on double polysaccharide film-coated microparticles for liquid products and their release behaviors

Bo Zheng [a] , Fengwei Xie [b] , Wenbei Situ [a] , Ling Chen [a*] , Xiaoxi Li [a*]

[a] *Ministry of Education Engineering Research Center of Starch & Protein Processing, Guangdong Province Key Laboratory for Green Processing of Natural Products and Product Safety, School of Food Science and Engineering, South China University of Technology, Guangzhou 510640, China*

[b] *School of Chemical Engineering, The University of Queensland, Brisbane, Qld 4072, Australia*

**Corresponding author.*

Email addresses: felchen@scut.edu.cn, xxlee@scut.edu.cn; Tel: +86 20 8711 3252

Abstract: A new carrier system for controlled release of immunologic peptides based on double polysaccharide film-coated microparticles (PCMPs) used with liquid products was developed. The release behavior of PCMPs was shown dependent on the thicknesses of the outer chitosan film and the inner resistant starch acetate (RSA) film. The *in-vitro* release results indicated that, with optimized polysaccharide coating thickness (RSA: 4–5%; chitosan: 6–7%), the release rate of Thymopoietin (TP5) was less than 30% before the microparticles reached the colon, and was 50% in the colon. Besides, the bioavailability of PCMPs was evaluated based on the cell proliferation and protein expression. Compared with the intraperitoneal injection or oral administration, the immunodeficient rats that were orally administrated with the yogurt containing TP5-loaded PCMPs with different storage times possessed a good colon-targeting behavior, higher ratios of CD4/CD8 and IgG expression, indicating the improvement in the TP5 immunologic function.

Keywords: liquid products; resistant starch acetate; chitosan; colon-targeting; controlled release; pH-responsiveness

Thymopoietin (PubChem CID: 50587); chitosan (PubChem CID: 71853); Fluorescein isothiocyanate isomer (PubChem CID: 18730)

1. Introduction

Compared with traditional food, functional food provides significant health benefits by regulating the physiological activity of the human body in addition to the nutritional and sensory functions (such as color, smell, and taste) (Boer, Urlings, & Bast, 2016). Given that, bioactive compounds are considered as the material basis of functional food (Izydorczyk et al., 2017). However, bioactive compounds such as TP5 can be easily destroyed during food processing (Andrés, Villanueva, & Tenorio, 2016; Buniowska, Carbonellcapella, Frigola, & Esteve, 2016) and storage (Gonzálezolivares, Añorvemorga, Castañedaovando, Contreraslópez, & Jaimezordaz, 2014; Grace et al., 2014), as well as in the human physiological environment (Lu, Zhang, Wang, & Chen, 2011; Zanjani, Tarzi, Sharifan, & Mohammadi, 2013). For the improved effectiveness and bioavailability of functional ingredients in food, it is significant to design a delivery system for bioactive compounds with the enhanced stability of bioactive compounds in both the pre-consumption and the human physiological environments.

Currently, liquid products systems such as yogurt play a major role in functional food (Tansey & Worsley, 2014). However, technical difficulties, resulting from the pH variation, the digestion enzymes, and the long transit time, are involved, which could negatively impact on the effective storage and the oral delivery of these bioactive compounds to the specific parts of the digestive tract as desired. To overcome these obstacles, it is important to design new controlled release delivery system for bioactive compounds that can be used in liquid products. The recent progress on the research of suitable carrier materials includes bacteria-degradable, pH-sensitive, pressure-sensitive, and time-dependent polymer coating films for the enhanced stability and bioavailability of bioactive compounds has provided renewed hope (Lin, Chen, & Luo, 2007; Maroni, Zema, Del Curto, Foppoli,

& Gazzaniga, 2012). Besides for effective storage, alginate (Champagne, 2006; Kailasapathy, 2006), oligosaccharide (K. N. Chen, Chen, Liu, Lin, & Chiu, 2005), whey protein (Lambert, Weinbreck, & Kleerebezem, 2008) and Arabia gum(A. Singh, Adak, Karmakar, & Banerjee, 2014) have been reported to be used as carrier materials for coating bioactive compounds used in different foods such as milk and fruit juice. Amylose and cacao oil have also been used as carrier materials in liquid products like oat beverage (Lahtinen, Ouwehand, Salminen, Forssell, & Myllärinen, 2007). Besides, suitable materials have been developed for controlled-release delivery systems (Constantin, Bucatariu, Doroftei, & Fundueanu, 2017; Deodhar, Adams, & Trewyn, 2016; Llopislorente, Lozanotorres, Bernardos, Martinezmanez, & Sancenón, 2017). Given the enormous interest in recent years towards maintaining biological activity, growing attention has been focused on many polysaccharides, such as cellulose, pectin, hyaluronic acid and inulin, in developing controlled release systems (Akhgari, Farahmand, Afrasiabi, Sadeghi, & Vandamme, 2006; Gurav, Kulkarni, Khan, & Shinde, 2016; W. He, Du, Cao, Xiang, & Fan, 2008; Ribeiro et al., 2016; Zhou, Wang, Hu, & Luo, 2016). However, in few studies so far, the development of release systems have addressed the dual purposes of the controlled release of bioactive compounds and the improvement in the storage stability of functional food. Thus, the paper reports our new efforts in developing controlled bioactive compound delivery systems with these double advantages.

Starch and chitosan are two polysaccharides that are biocompatible and biodegradable and have already been widely used in different foods (Z. He et al., 2017; J. Singh, Kaur, & Mccarthy, 2007). Starch can be modified easily to overcome its native hydrophilicity and limitations against the acid and enzymes in the gastrointestinal tract (Bayat et al.; L. Chen, Li, Li, & Guo, 2007; Sharma, Yadav, & Ritika, 2007). The modified starch may avoid being hydrolyzed in the small intestine but can still

be degraded by the microorganisms in the colon (Pu, Chen, & Li, 2011). It has been reported by our group that resistant starch acetate (RSA) can be used as a potential carrier for oral colon-specific delivery (Bie, Chen, Li, & Li, 2016; L. Chen et al., 2007; Li, Peng, Ling, & Long, 2011; Xiao, Liu, & Sun, 2011). On the other hand, the dissolution and structure of chitosan are highly responsive to pH in the upper GI tract (Bayat et al., 2008; Pan et al., 2016) and therefore can also be a promising carrier material. Moreover, by adjusting the molecular structure and thus the film forming properties of chitosan, the chitosan film can absorb water to form a gel in a weak-acid environment and dissolve in a strong-acid environment. Therefore, by adjusting the digestion resistibility of starch and the pH-responsiveness of chitosan based on molecular design, it is possible to develop a complex polysaccharide material that can be used to construct a controlled-release delivery system for liquid products.

In this study, colon-targeted controlled-delivery systems based on double polysaccharide film-coated microparticles (PCMPs) for yogurt were designed using RSA (the degree of substitution: 1.9), which had digestion resistibility, and chitosan (M_w: 1.5×10^5 g/mol), which was pH-responsive, as coating materials. TP5-loaded PCMPs were prepared, in which TP5 was used as a model bioactive compound. Moreover, the release behavior during yogurt storage and *in-vitro* simulated GI transportation were investigated, with the variation in the polysaccharide coating thicknesses. Furthermore, the *in-vivo* effectiveness of TP5-loaded PCMPs was evaluated by tissue immunocytochemistry, and the *in-vivo* TP5 bioactivity was studied in immune model rats.

2. Materials and methods

2.1 Chemicals and reagents

RSA with the degree of acetyl substitution (DS) of 1.9 was synthesized from a high-amylose starch (50% amylose content, from Penford, Australia) using the method as previously described (Zhang, Chen, Zhao, & Li, 2013). Chitosan (M_w: 1.5×10^5 g/mol) was purchased from Kayon Biological Technology Co., Ltd. (Shanghai, China). Lactic acid bacteria powder was supplied by Chuanxiu Technology Co., Ltd. (Beijing, China). Sterilized pure whole milk was provided by Yili Industrial Group Limited by Share Ltd. (Inner Mongolia, China). Microcrystalline cellulose (SH-102) was purchased from Anhui Shanhe Medicinal Accessory Material Co., Ltd. (Huainan, China). TP5 was supplied by GL Biology and Chemistry Co., Ltd. (Shanghai, China). FITC, red blood cell lysis, FITC anticat CD3, PE anticat CD8a, APC anticat CD4, and anticoagulation tubes were purchased from BD Bioscience Co., Ltd. (USA). The ELISA Kit for Immunoglobulin G (IgG) was supplied by Chenglin Biological Technology Co., Ltd. (Beijing, China) Cyclophosphamide was purchased from Aladdin Co., Ltd. (Shanghai, China).

2.2 Preparation of RSA films

The RSA films were prepared by a flow-casting method. RSA was suspended in acetone and stirred for 3 min to make it dissolve completely. An RSA solution was then prepared, with triacetin as a plasticizer at a content of 25% (w/w) of RSA. The mixture was stirred for another 8 h, before casting in a polypropylene plate with a diameter of 14 cm. The cast films were dried in an oven at 45 °C for 12 h, which could then be manually detached from the plate. Finally, 1 g of the RSA film

was added to 100 g of a fresh fermented yogurt, which was mixed evenly and then stored in a 4 °C refrigerator for different days (1,7,13,19 days) based on the quality guarantee period of yogurt.

2.3 X-ray diffraction(XRD)

Crystalline structure was identified using an X-ray diffractometer (X'Pert Prox, Panalytial, The Netherlands) operated at 40 kV and 40 mA with Cu-Ka radiation (0.1542 nm). The diffractograms of the samples were acquired at an angular angle (2θ) range of 4°to 40° with a step size of 0.033° and a counting time of 4 s for each step. The ratio of the upper area (crystalline portion) to the total diffraction area (based on a linear baseline) was taken as the relative crystallinity using the software MDI Jade 6.0. The relative crystallinity of all these samples was calculated using the MDI Jade software (Nara & Komiya, 1983).

2.4 Dynamic mechanical properties of RSA films

The dynamic mechanical properties of RSA films were investigated by a PerkinElmer Diamond dynamic mechanical analyzer (DMA) (PerkinElmer, Inc., Waltham, MA, USA) using the tensile mode. Rectangular specimens with a dimension of 40 (length) × 10 (width) mm were cut from the central part of the films using a cutting mold. A frequency of 1.0 Hz was used. The storage modulus (E'), loss modulus (E''), mechanical loss factor (tan δ) were recorded. The temperature scanning proceeded from 30 °C up to 90 °C with a rate of 2 °C/min. Triple tests were carried out to each sample to ensure data reliability.

2.5 Preparation of polysaccharide-coated microparticles (PCMPs).

TP5 was used as a model bioactive compound. TP5-loaded microparticles (containing microcrystalline cellulose and starch in the ratio of 3:1) were obtained via extrusion-spheronization

(Pu et al., 2011). During the extrusion-spheronization, the temperature was kept at 5–10 °C to maintain the activity of TP5.

The microparticle cores loaded with TP5 were then coated with RSA, and then with chitosan, using a bottom spray fluid bed coater (Mini-XYT; Xinyite Technology Co., Shenzhen, China) until a certain weight (thickness) of the coated film was achieved, which was representative of the dry weight gain of the microparticles (Pu et al., 2011). In this way, seven samples of double polysaccharide film-coated microparticles (PCMPs) were prepared: Type I: RSA 2.65%, chitosan 8.73%; Type II: RSA 4.15%, chitosan 9.56%; Type III: RSA 7.89%, chitosan 8.26%; Type IV: RSA 4.45%, chitosan 1.47%; Type V: RSA 4.45%，chitosan 3.87%; Type VI: RSA 5.14%, chitosan 7.07%; Type VII: RSA 4.15%, chitosan 0%) The process parameters were: the inlet temperature at 44±1 °C; temperature of TP5-loaded microparticles at 30±2 °C; spray rate of coating dispersion at 0.7–0.8 mL/min; atomization pressure of 0.15 MPa; and fluidization pressure at 0.15 MPa. PCMPs were finally dried in an oven at 45 °C for 24 h. 1 g of PCMPs were added into 100 g of a fresh fermented yogurt, mixed evenly and then stored in a 4°C refrigerator for 1 to 19 days for the establishment of liquid products delivery systems.

2.6 Release tests during yogurt storage

After stored in the yogurt for different times, PCMPs were taken out and washed with distilled water. Furthermore, PCMPs were soaked and fully dissolved in a hydrochloric acid solution of pH 1.2, then ground and filtered. The filtrate was diluted with water to 100 mL. The amount of TP5 released from the PCMPs was determined using a UV spectrophotometer at a wavelength of 275 nm.

2.7 *In-vitro* release tests

The *in-vitro* release behavior of PCMPs was studied according to the China Pharmacopoeia (2015) dissolution method using a dissolution rate test apparatus (J. Chen et al., 2016). 1 g of PCMPs stored in yogurt for different times was taken out and washed with distilled water twice, then immersed in the simulated gastric fluid (SGF) for the first 2 h, in the simulated intestinal fluid (SIF) for another 6 h, and afterward in the simulated colonic fluid (SCF) for an additional 40 h, in sequence, all at 37±0.5 °C with agitation using a paddle at a rotation speed of 100 rpm by an intelligent medicine dissolving instrument (RCZ-8B, Tianjin Tianda Tianfa Technology Co., Ltd., Tianjin, China) (Pu et al., 2011; Situ, Chen, Wang, & Li, 2014). When the simulated digestive fluid changed, PCMPs were filtered by filter paper under vacuum, washed with distilled water twice, and then put into the following simulated digestive fluid. At appropriated time intervals, 5 mL of the sample was collected from the simulated digestive tract fluid for analysis every one hour, and the amount of TP5 released from the PCMPs was determined using a UV spectrophotometer at a wavelength of 275 nm.

2.8 *In-vitro* fluorescent imaging

Five SPF-grade nude mice (7 to 8 weeks old, all females, Vital River Laboratory Animal Technology Co., Ltd., Beijing, China) weighing approximately 12−14 g were fasted for 12 h before the study. The yogurt containing FITC-labeled PCMPs after storage for different times (1 and 13 days) were orally administrated to the stomach via polyethylene tubing under light ether anesthesia. Meanwhile, three blank groups containing PBS buffer, the yogurt, and FITC-labeled PCMPs were imaged for comparison. The PCMPs were dosed at 0.2 mg per gram of body weight. At 10, 15, 30,

45, 60, 90, 120, 150 and 180 min after oral administration, the fluorescence intensity and transmission of the PCMPs in the nude mice were observed by an small-animal whole-body *in-vivo* imaging system (IVIS 200, Xenogen Corp., Alameda, CA, USA) at 445−490 nm of exciting light and 515−575 nm of emitted light with an exposure time of 5 s. The nude mice were anesthetized by isoflurane before being photographed.

2.9 TP5 bioactivity

Thirty female rats were randomly divided into six groups for the pharmacodynamics study. The ratio of CD4/CD8 in the peripheral blood of each rat was determined as an “internal control” before implantation. The first group of rats were orally administrated with PBS buffer, 2 mL/kg/day, and the second to the sixth group were immunosuppressed by intraperitoneal injection of cyclophosphamide (CTX) at a dosage of 35 mg/kg/day. After CTX treatment for 3 days, if the ratio of CD4/CD8 was beyond the range of 1.5–2.0, the immune deficiency model was considred to be established successfully. After the establishment of the model of the immune deficiency rats, the second group of rats was orally administrated with PBS buffer, 2 mL/kg/day, as an immune suppression control group. In the third to fifth group, each rat was respectively orally administrated with the yogurt without TP5 microparticles, with the TP5 solution (12 mg/kg/day), and with the yogurt containing TP5-loaded PCMPs after storing 13 days (the dosage of TP5 was 12 mg/kg/day). Meanwhile, in the sixth group, each rat was given TP5 solution by intraperitoneal injection, 12mg/kg/day. A 200μL aliquot of blood was collected into a heparinized tube via the caudal vein 2, 5, 8, 12 and 16 days after implantation and stored at 4 °C. All the samples were analyzed by flow cytometry within 15 min.

2.10 Flow cytometric analysis of peripheral blood

The lymphocyte populations in the peripheral blood were analyzed by dual-color flow cytometry. An antibody solution (1 mL) containing 1% serum was transferred to a new centrifuge tube coated with aluminum foil and then mixed with anti-rat CD4 (25 μL) and anti-rat CD8a (25 μL). Blood samples (200 μL) were washed with PBS by centrifugation at 1500 rpm for 10 min and then mixed with the antibody solution (22 μL). After incubation in the dark at room temperature for 30 min, red blood cell lysis buffer (200 μL) was added to the blood sample, incubated in the dark at room temperature for 10 min, and washed twice with PBS by centrifugation at 1500rpm for 10 min. Data was analyzed by the CELL Quest software and represented as dual-parameter density plots.

2.11 Enzyme-linked immunosorbent assay (ELISA) analysis of serum antibodies

The concentrations of serum antigen-specific IgG in individual animals were analyzed by ELISA, according to the manufacturer's instructions (Bethyl, USA). Individual serum samples at 1:1–1:5 dilutions were tested in triplicate and incubated at 37 °C for 30 min. Subsequently, the bound antibodies were incubated with horseradish peroxidase (HRP)-conjugated goat anti-rat IgG (1:100) (Bethyl, USA) at 37 °C for 30min. After washing, the bound HRP-conjugated secondary antibodies were detected with a tetramethylbenzidine substrate. The reaction was stopped by adding 50 μL/well of 1 M H_2SO_4, and the optical density was measured at 450 nm.

2.12 Statistical Analysis

All data were subjected to statistical analysis using the SPSS 16.0 statistical package and were presented as the mean ± standard deviation (±SD). Differences between groups were estimated by

analysis of *t*-test, and $P < 0.01$ was considered to indicate a statistically significant difference between two groups.

3. Results and Discussion

3.1 Changes in crystalline structure of RSA film during Yogurt storage

Figure 1a shows the wide-angle XRD spectra of the native RSA film and four samples with the RSA film in the yogurt after storage for different times (1, 7, 13, 19 days). It can be seen that the crystalline structure (related to the V-type diffraction pattern) of the RSA film stored in the yogurt for different days was the same as the native RSA film. For these 5 samples, the relative crystallinity values were calculated to be 9.2, 10.6, 11.1, 11.6, and 12.0, respectively. The relative crystallinity was slightly increased with a longer storage time. This was due to the influence of acid and water molecules in the liquid products, which promoted the degradation and rearrangement of RSA chains. As a result, the aggregation structure of RSA films was changed, and the ordering of RSA chains was increased.

3.2 Changes in dynamic thermal-mechanical properties of RSA film during storage in yogurt

The dynamic thermal-mechanical properties of RSA film as affected by the yogurt were investigated by DMA, and the results are shown in **Fig. 1 b-d**. It could be seen that when all samples were at a low temperature, the E' values were in the range of 4.0×10^8 – 7.0×10^8 Pa, indicating that the films had strong rigidity. With the increased temperature, E' decreased all along, but tan δ firstly increased and then decreased. The peak of a tan δ curve describes the glass transition temperature (T_g)

of materials (Zhu, Li, Huang, Chen, & Li, 2013). Here, the storage in the yogurt influenced T_g of the films significantly, with T_g increased with a longer storage time.

During storage in the yogurt, with the presence of acid and water, the ordering of RSA chains was improved by rearrangements, leading to the increased crystallinity of the RSA film. Moreover, the infiltration of water into the film allowed the interactions between RSA chains and water molecules through hydrogen bonding. These interactions could restrict the movement of starch molecules and the rigidity of the film, as reflected by increased E' and T_g. The longer the storage time, the higher were E' and T_g. A longer storage time could also result in embrittlement of the film.

3.3 Effect of coating thicknesses on the release behavior of PCMPs during storage in yogurt

The PCMPs delivery systems were obtained using TP5 as the model bioactive compound, and the effect of film coating thicknesses on the TP5 release behavior of PCMPs in the yogurt and in the simulated human GI tract was investigated. Firstly, PCMPs were coated with three different thicknesses of RSA but with a similar thickness of chitosan (as shown in **Method 2.5** Types I-III).

The release behavior of these three PCMP samples in the yogurt was illustrated in f**igure 2a**. It can be seen that, for each sample, the release rate of PCMPs was increased with the storage time. Comparing the cumulative release percentages of TP5 from the three PCMP samples, it was suggested that under the same storage time and with the same coating thickness of chitosan, the release rate, which reflected the amount of TP5 in yogurt, was decreased with the increased thickness of the inner RSA coating. Besides, after storage for 1 and 22 days in the yogurt, PCMP Sample 1 released 16.41% and 29.69% of TP5, respectively. This was mainly due to the loose film of RSA.

Based on the results of XRD and DMA analysis, the rigidity of RSA film was increased during storage in the yogurt, which made the RSA film brittle. In this way, TP5 in PCMPs was released through the gel formed by the outer chitosan layer after storage, which prevented the intrusion by the surrounding liquid products. Thus, the coating thickness of the inner RSA film was a determinant factor influencing the release behavior of the bioactive compounds during storage in liquid products.

3.4 Effect of polysaccharide coating thicknesses on the release behavior of PCMPs in the simulated human GI tract

The release behaviors of three PCMP samples in the simulated human GI tract after storage in the yogurt for 1, 7, 13, and 19 days was shown in **Figure 2b-e**. It can be seen that the release rate for TP5 in every PCMP sample was increased with the increased storage time in the yogurt. Besides, the release rate for TP5 was decreased with a greater thickness of the RSA coating. It can be proposed that when PCMPs entered the simulated GI tract environment, the time for the dissolution of chitosan in gastric acid delayed the release of TP5 in the upper GI tract. After the dissolution of the outer chitosan layer, the inner RSA film still resisted the erosion by digestive enzymes and gastric acid in the small intestine, which allowed the targeting delivery of TP5 to the colon, These dual functions could maximize the biological activity of TP5.

To investigate the effect of chitosan coating thickness on the release rate of the bioactive compound, PCMPs were coated with three different thickness of chitosan (as shown in **Method 2.5** Types IV–VI).The release behaviors of these three PCMP samples in the simulated human GI tract were shown in **Figure 2f-i**. The release of TP5 in the colon could be adjusted by the coating thickness of the outer chitosan layer. When the coating thickness of the inner RSA layer and the outer

chitosan layer were between 4–5% and 6–7%, respectively, the cumulative TP5 release rates in the upper GI tract could be controlled to be about 30% and 80% in the colon after storage in the yogurt for 19 days. This meant that the colon-targeted delivery of TP5 was achieved.

Table 1 shows the release rates of different PCMP samples after storage in the yogurt for various days. After storage, part of TP5 had already been released at release time 0 h. Moreover, the release rate of PCMPs in the simulated GI tract was significantly increased. It can be seen that with a similar coating thickness of RSA, PCMP samples had similar release rate when stored in the yogurt, while they had different release rate in the GI tract. For RSA-coated microparticles, 39.08% and 50.74% of TP5 were released in the upper GI tract after storage in the yogurt for 1 and 19 days, respectively, while PCMPs released 16.26–29.78% and 24.08–31.94% after storage for the same time periods, respectively. These results further suggested that the outer chitosan layer avoided the release of TP5 before reaching the colon. Furthermore, a certain thickness of chitosan helped restrict the release of TP5 before the colon, which improved the bioavailability of bioactive compounds.

3.5 Release mechanism of liquid products delivery system with pH responsiveness and colon-targeted release

Based on the data discussed above, a release mechanism of the delivery systems based on liquid products with pH responsiveness and colon-targeted release is proposed here as shown in **Figure 3**.

In the beginning, the bioactive compounds were evenly distributed throughout PCMPs with RSA as the inner layer and chitosan as the outer layer (**Figure 3 I**).

When PCMPs were stored in the yogurt, the outer chitosan layer absorbed water. With the increased storage time, the swelling of the chitosan layer led to the formation of a gel structure

around the particle (**Figure 3 II**). The disintegration of the chitosan layer allowed the water and other substances in the yogurt to be gradually in direct contact with the RSA layer. However, RSA was capable of resisting water intrusion from the yogurt because of its certain hydrophobicity (**Figure 3 III**).

During the storage in the yogurt, the ordering of RSA chains was increased through molecular rearrangements. Moreover, because of the infiltration of water molecules from the surrounding liquid products for the interaction and hydrogen-bonding formation with starch chains, the movement of starch chains was restricted, leading to the increased rigidity and embrittlement of the film. If the RSA layer was not thick enough, with a longer storage time, a small amount of TP5 would be released from the PCMPs into the surrounding yogurt through the chitosan gel layer. Therefore, the swelling capacity of the chitosan film, together with the hydrophobicity of the RSA layer, maintained the stability of the bioactive compound in the liquid products during storage.

After transported from the yogurt to the simulated human GI tract, PCMPs were firstly in contact with low pH gastric juice. The low pH allowed the outer chitosan gel layer to be dissolved gradually due to a pair of non-shared electrons on the nitrogen atom of the amino group of chitosan, which contributed to the combination with a hydrogen ion from the gastric juice (**Figure 3 IV**). Meanwhile, gastric juice also began to reach the inner RSA layer. Nevertheless, owing to the high DS of RSA and thus the resistant starch content, the inner RSA layer was intact, and the release of bioactive compounds was prevented. After PCMPs had been transported to the small intestine, the chitosan gel layer was mostly eliminated. The integrity of the RSA layer was mostly kept but could contain minor damages, which allowed the release of the bioactive compound (**Figure 3 V**).

After the PDMCs had been transported to the colon, the colonic microbial fermentation resulted in holes in the RSA coating layer, which allowed the release of the bioactive compound to the surrounding colon environment (**Figure 3 VI**).

In this scheme, RSA had a significant number of acetyl groups, which formed steric hindrance and resist to digestion. Besides, a certain degree of hydrophobicity of RSA was helpful to resist the degradation by the acid and various digestive enzymes initially, whereas RSA could still be fermented by colonic microflora.

3.6 *In-vivo* colonic targeting and bioadhesion of PCMPs

Using *in-vivo* fluorescent imaging observed by a small-animal whole-body *in-vivo* imaging system, the oral colonic targeting capability of FITC-labeled PCMPs was studied. **Figure 4** shows the distribution of PCMPs in different parts of the GI tract of nude mice at different times after oral administration. Before administration, no fluorescence was shown in the nude mice (**Figure 4a**). With the increased transit time after the oral administration of PCMPs (from 10 to 45 min), the fluorescence spots moved from the stomach to the small intestine and then to the colon. At 45 min after oral administration, all the fluorescence spots concentrated in the colon, indicating that PCMPs had reached the colon (**Figure 4d−i**). As the transit time was prolonged further, the fluorescence intensity at the colon was gradually increased, and the fluorescence spots were enlarged, which could be due to the release of FITC from PCMPs. The results here indicated good colonic targeting of PCMPs for liquid products.

From **Figure 4**, it was seen that after oral administration, the FITC-labeled PCMPs that were stored in the yogurt for 1 and 13 days showed some differences in the time and intensity of

fluorescent spots in the body. At 15 min after oral administration of the FTIC-labeled PCMPs that were stored in the yogurt for 13 days, the fluorescent spots appeared in the small intestine, and the intensity of spot increased gradually for the growing time. At 45 min, the PCMPs that were stored in the yogurt for 13 days had been transported to the upper colon, and the intensity of spots was brighter than those without storage or with only one-day storage in the yogurt. This result indicated that the storage time for PCMPs in liquid products had little influence on colon-targeted delivery.

3.7 Bioavailability of thymus peptide five (TP5)

3.7.1 Effect of TP5 on $CD4^+$ and $CD8^+$ cells

TP5 is a natural polypeptide that promotes the growth of thymus(Janway, 1992). However, if directly injected or orally administered, TP5 could be degraded easily in the animal body, which limited its function on T-lymphocytes (Amin et al., 2016). As **Figure 5a-d** shows, the populations of $CD4^+$ and $CD8^+$ cells in rats that were orally administrated with the yogurt containing TP5-loaded PCMPs with different storage time for 7 days were higher than those for the other groups.

From **Figure 5e-h** it can be seen that as the time increased for oral administration, the proportions of $CD4^+$ or $CD8^+$ cells to the total lymphocytes in immune deficiency rats were increased gradually. Also, the proportions reached the maxima on the first day after oral administration. Subsequently, with the end of the oral administration, the proportions of $CD4^+$ and $CD8^+$ cells to the total lymphocytes were decreased gradually.

Table 2 presents the ratio of CD4/CD8 in immune model rats after different days of oral administration or injection of TP5 solution with the same dosage of TP5. The ratio of CD4/CD8 in the model control group, the TP5 oral administration group, and the TP5 injection group were all less

than 1.5. In the TP5 PCMPs yogurt group, the ratio of CD4/CD8 was significantly increased with the increased time ($P < 0.01$). At Day 8, the ratio reached the maximum of 1.52, but still within the normal range. When the time was further extended, the ratio was decreased gradually, which was similar to the model control group. Moreover, there was no significant difference between the model control group, the TP5 oral administration group, and the TP5 injection group. These results showed the pH-responsiveness and the colon-targeted controlled-release performance of PCMPs. After stored in the yogurt and transported into the rat GI tract, PCMPs released TP5 mainly in the colon. Also, there were plenty of lymphoid tissue in the colon, which could directly absorb and utilize proteins such as TP5. This mechanism could prevent the adverse effect of the liver on the bioactive compound, and allowed TP5 to be absorbed in the colon to make it act on the targeted cells, which improved the immunological activity of the cells.

Figure 6a-b shows the results regarding the effect of the dosage of oral administration of the TP5-loaded PDMCs received by immune model rats on the CD4/CD8 value. After 7 days of oral administration, the CD4/CD8 ratio of the TP5 high-dosage group was significantly increased, which was even close to the normal range, and better than that of the TP5 injection group. Besides, the CD4/CD8 ratio was slightly higher in the rats that were orally administrated with the TP5-loaded PCMPs that were stored in the yogurt for 19 days than that with the TP5-loaded PCMPs that were stored in the yogurt for 7 days.

3.7.2 Effect of TP5 on rat immunoglobulin (IgG) expression

Table 2 also shows the results regarding the effect of PCMPs on the change in the TP5 concentration in immune deficiency model rats. After modeling, the content of IgG in the blood of

rats in each group was similar (9.50–12.33 mg/mL) without significant difference. Furthermore, with a prolonged time after oral administration of the yogurt containing PCMPs, the content of IgG in the blood of rats was increased gradually, and reached the maximum at Day 12. This was because the TP5 that was released in the colon was absorbed by the body of the rats, which improved the immunity of T cells and provided the relevant auxiliary stimulation signal and cytokines, thus promoting the production of antibodies for B cells. Compared with the TP5 PCMPs yogurt group, the TP5 oral administration group and the TP5 injection group had a lower content of IgG in the blood, though there was an improvement within their individual groups with time.

Figure 6c-d shows the effect of dosage of oral administration of TP5-loaded PCMCs on the change in the IgG expression in immune model rats. It could be seen that the IgG expression of immune model rats with yogurt treatment contained the different dosage of TP5-loaded PCMPs was higher (18.6−29.7 mmol/L) than those of the normal group, the control group, and TP5 injection group. As mentioned earlier, B cell activation requires costimulatory signals and cytokines provided by T cells. Thus, it was reasonable to see that, regardless of the dosage of TP5, TP5 in PCMPs could be absorbed by rats and then acted on T cells, which led to the recovery of the cellular immune activity and improved the immunity of rats eventually.

4. Conclusion

This research is focused on the development of a colon-targeted controlled release system based on PCMPs for liquid products. The results indicated that both the storage stability and the colon-targeted controlled release performance of the bioactive compound, TP5, could be achieved with PCMPs with 4–5% and 6–7% of the inner RSA film and the outer chitosan film, respectively.

413 The release rate of TP5 was 50% in the colon, which improved the bioavailability of immune peptide.
414 Thus, this work has provided a new approach for enhancing the bioavailability of functional foods.

415 Potential conflict of interest statement

416 The authors declare no competing financial interest.

417 Acknowledgement

418 This research has been financially supported under the National Natural Science Foundation of
419 China (NSFC)-Guangdong Joint Foundation Key Project (U1501214), YangFan Innovative and
420 Entrepreneurial Research Team Project (2014YT02S029), the R&D Projects of Guangdong Province
421 (2014B090904047), the Science and Technology Program of Guangzhou (201607010109), the Key
422 R&D Projects of Zhongshan (2014A2FC217)，the innovative projects for Universities in Guangdong
423 Province (2015KTSCX006), and the Fundamental Research Funds for the Central Universities
424 (2015ZZ106).

425 References

426 Akhgari, A., Farahmand, F., Afrasiabi, G. H., Sadeghi, F., & Vandamme, T. F. (2006). Permeability
427 and swelling studies on free films containing inulin in combination with different
428 polymethacrylates aimed for colonic drug delivery. *European Journal of Pharmaceutical*
429 *Sciences, 28*(4), 307-314.
430 Amin, N. D., Zheng, Y., Bk, B., Shukla, V., Skuntz, S., Grant, P., Pant, H. C. (2016). The interaction
431 of Munc 18 (p67) with the p10 domain of p35 protects in vivo Cdk5/p35 activity from
432 inhibition by TFP5, a peptide derived from p35. *Molecular Biology of the Cell, 27*(21).
433 Andrés, V., Villanueva, M. J., & Tenorio, M. D. (2016). The effect of high-pressure processing on
434 colour, bioactive compounds, and antioxidant activity in smoothies during refrigerated
435 storage. *Food Chemistry, 196*, 328-335.

436 Bayat, A., Dorkoosh, F. A., Dehpour, A. R., Moezi, L., Larijani, B., Junginger, H. E., & Rafieetehrani,
437 M. (2008). Nanoparticles of quaternized chitosan derivatives as a carrier for colon delivery of
438 insulin: ex vivo and in vivo studies. *International Journal of Pharmaceutics, 356*(356),
439 259-266.
440 Bie, P., Chen, L., Li, X., & Li, L. (2016). Characterization of concanavalin A-conjugated resistant
441 starch acetate bioadhesive film for oral colon-targeting microcapsule delivery system.
442 *Industrial Crops & Products, 84*, 320-329.
443 Boer, A. D., Urlings, M. J. E., & Bast, A. (2016). Active ingredients leading in health claims on
444 functional foods. *Journal of Functional Foods, 20*, 587-593.
445 Buniowska, M., Carbonellcapella, J. M., Frigola, A., & Esteve, M. J. (2016). Bioaccessibility of
446 bioactive compounds after non-thermal processing of an exotic fruit juice blend sweetened
447 with Stevia rebaudiana. *Food Chemistry*.
448 Champagne, C. P. (2006). Starter Cultures Biotechnology: The Production of Concentrated Lactic
449 Cultures in Alginate Beads and Their Applications in the Nutraceutical and Food Industries
450 (Review paper). *Chemical Industry & Chemical Engineering Quarterly, 12*(1), 11-17.
451 Chen, J., Zhang, K., Yang, Z. Q., Wang, X. L., Pan, F., School, G., & University, T. M. (2016).
452 Research of dissolution determination method of dexlansoprazole sustained-release capsules.
453 *Chinese Journal of New Drugs*.
454 Chen, K. N., Chen, M. J., Liu, J. R., Lin, C. W., & Chiu, H. Y. (2005). Optimization of incorporated
455 prebiotics as coating materials for probiotic microencapsulation. *Journal of Food Science,*
456 *70*(5), M260-M266.
457 Chen, L., Li, X., Li, L., & Guo, S. (2007). Acetylated starch-based biodegradable materials with
458 potential biomedical applications as drug delivery systems. *Current Applied Physics, 7*,
459 e90-e93.
460 Constantin, M., Bucatariu, S. M., Doroftei, F., & Fundueanu, G. (2017). Smart composite materials
461 based on chitosan microspheres embedded in thermosensitive hydrogel for controlled
462 delivery of drugs. *Carbohydrate Polymers, 157*, 493-502.
463 Deodhar, G. V., Adams, M. L., & Trewyn, B. G. (2016). Controlled release and intracellular protein
464 delivery from mesoporous silica nanoparticles. *Biotechnology Journal*.
465 Gonzálezolivares, L. G., Añorvemorga, J., Castañedaovando, A., Contreraslópez, E., & Jaimezordaz,

J. (2014). Peptide separation of commercial fermented milk during refrigerated storage. *Ciência E Tecnologia De Alimentos, 34*(4), 674-679.

Grace, M. H., Yousef, G. G., Gustafson, S. J., Truong, V. D., Yencho, G. C., & Lila, M. A. (2014). Phytochemical changes in phenolics, anthocyanins, ascorbic acid, and carotenoids associated with sweetpotato storage and impacts on bioactive properties. *Food Chemistry, 145*(4), 717-724.

Gurav, D. D., Kulkarni, A. S., Khan, A., & Shinde, V. S. (2016). pH-responsive targeted and controlled doxorubicin delivery using hyaluronic acid nanocarriers. *Colloids & Surfaces B Biointerfaces, 143*, 352.

He, W., Du, Q., Cao, D. Y., Xiang, B., & Fan, L. F. (2008). Study on colon-specific pectin/ethylcellulose film-coated 5-fluorouracil pellets in rats. *Int J Pharm., 348*(1-2), 35-45.

He, Z., Santos, J. L., Tian, H., Huang, H., Hu, Y., Liu, L., Mao, H.-Q. (2017). Scalable fabrication of size-controlled chitosan nanoparticles for oral delivery of insulin. *Biomaterials*, 28–41.

Izydorczyk, M. S., McMillan, T., Bazin, S., Kletke, J., Dushnicky, L., Dexter, J., Rossnagel, B. (2017). Milling of Canadian oats and barley for functional food ingredients: Oat bran and barley fibre-rich fractions. *Canadian Journal of Plant Science, 94*(3), 573-586.

Janway, C. A. (1992). The T cell receptor as a multicomponent signalling machine: CD4/CD8 coreceptors and CD45 in T cell activation. *Annual Review of Immunology, 10*(10), 645-674.

Kailasapathy, K. (2006). Survival of free and encapsulated probiotic bacteria and their effect on the sensory properties of yoghurt. *LWT - Food Science and Technology, 39*(10), 1221-1227.

Lahtinen, S. J., Ouwehand, A. C., Salminen, S. J., Forssell, P., & Myllärinen, P. (2007). Effect of starch- and lipid-based encapsulation on the culturability of two Bifidobacterium longum strains. *Letters in Applied Microbiology, 44*(5), 500-505.

Lambert, J. M., Weinbreck, F., & Kleerebezem, M. (2008). In vitro analysis of protection of the enzyme bile salt hydrolase against enteric conditions by whey protein-gum arabic microencapsulation. *Journal of Agricultural & Food Chemistry, 56*(18), 8360.

Li, X., Peng, L., Ling, C., & Long, Y. (2011). Effect of resistant starch film properties on the colon-targeting release of drug from coated pellets. *Journal of Controlled Release, 152 Suppl 1*(1), e5.

Lin, Y., Chen, Q., & Luo, H. (2007). Preparation and characterization of

N-(2-carboxybenzyl)chitosan as a potential pH-sensitive hydrogel for drug delivery. *Carbohydrate Research, 342*(1), 87-95.

Llopislorente, A., Lozanotorres, B., Bernardos, A., Martinezmanez, R., & Sancenón, F. (2017). Mesoporous Silica Materials for Controlled Delivery based on Enzymes. *Journal of Materials Chemistry B*.

Lu, H. W., Zhang, L. M., Wang, C., & Chen, R. F. (2011). Preparation and properties of new micellar drug carriers based on hydrophobically modified amylopectin. *Carbohydrate Polymers, 83*(4), 1499-1506.

Maroni, A., Zema, L., Del Curto, M. D., Foppoli, A., & Gazzaniga, A. (2012). Oral colon delivery of insulin with the aid of functional adjuvants. *Advanced Drug Delivery Reviews, 64*(6), 540-556.

Nara, S., & Komiya, T. (1983). Studies on the Relationship Between Water-satured State and Crystallinity by the Diffraction Method for Moistened Potato Starch. *Starch - Stärke, 35*(12), 407-410.

Pan, Q., Lv, Y., Williams, G. R., Tao, L., Yang, H., Li, H., & Zhu, L. (2016). Lactobionic acid and carboxymethyl chitosan functionalized graphene oxide nanocomposites as targeted anticancer drug delivery systems. *Carbohydrate Polymers, 151*, 812.

Pu, H., Chen, L., & Li, X. (2011). An Oral Colon-Targeting Controlled Release System Based on Resistant Starch Acetate: Synthetization, Characterization, and Preparation of Film-Coating Pellets. *Journal of Agricultural & Food Chemistry, 59*(10), 5738-5745.

Ribeiro, S. D., Guimes, R. F., Meneguin, A. B., Prezotti, F. G., Boni, F. I., Cury, B. S. F., & Gremião, M. P. D. (2016). Cellulose triacetate films obtained from sugarcane bagasse: Evaluation as coating and mucoadhesive material for drug delivery systems. *Carbohydrate Polymers, 152*, 764.

Sharma, A., Yadav, B. S., & Ritika. (2007). Resistant Starch: Physiological Roles and Food Applications. *Food Reviews International, 24*(2), 193-234.

Singh, A., Adak, S., Karmakar, S., & Banerjee, R. (2014). Impact of Processing Condition on Nutraceutical Potency of Soy Whey Hydrolysate. *Journal of Food Quality, 37*(37), 403–414.

Singh, J., Kaur, L., & Mccarthy, O. J. (2007). Factors influencing the physico-chemical, morphological, thermal and rheological properties of some chemically modified starches for

food applications—A review. *Food Hydrocolloids, 21*(1), 1-22.

Situ, W., Chen, L., Wang, X., & Li, X. (2014). Resistant Starch Film-Coated Microparticles for an Oral Colon-Specific Polypeptide Delivery System and Its Release Behaviors. *Journal of Agricultural & Food Chemistry, 62*(16), 3599.

Tansey, G., & Worsley, A. (2014). *The Food System*: Routledge.

Xiao, L., Liu, C., & Sun, Y. (2011). A novel oral colon-targeting drug delivery system based on resistant starch acetate. *Journal of Controlled Release, 152 Suppl 1*(1), e51-52.

Zanjani, M. A. K., Tarzi, B. G., Sharifan, A., & Mohammadi, N. (2013). Microencapsulation of Probiotics by Calcium Alginate-gelatinized Starch with Chitosan Coating and Evaluation of Survival in Simulated Human Gastro-intestinal Condition. *Iranian Journal of Pharmaceutical Research, 13*(13), 843-852.

Zhang, B., Chen, L., Zhao, Y., & Li, X. (2013). Structure and enzymatic resistivity of debranched high temperature–pressure treated high-amylose corn starch. *Journal of Cereal Science, 57*(3), 348–355.

Zhou, M., Wang, T., Hu, Q., & Luo, Y. (2016). Low density lipoprotein/pectin complex nanogels as potential oral delivery vehicles for curcumin. *Food Hydrocolloids, 57*, 20-29.

Zhu, J., Li, X., Huang, C., Chen, L., & Li, L. (2013). Plasticization effect of triacetin on structure and properties of starch ester film. *Carbohydrate Polymers, 94*(2), 874-881.

Figure captions

Figure 1. XRD pattern and DMA results of the RSA film in yogurt for different storage times (a: XRD patterns; b: storage modulus (E'); c: loss modulus (E''); d: loss angle tangent (tan δ)).

Figure 2. a: Release behaviors of PCMPs during storage in yogurt; b-i: Release behaviors of PCMPs in the GI tract after storage in yogurt for different days (b and f: 1 day; c and g: 7 days; d and h: 13 days; e and i: 19 days).

Figure 3. Release mechanism of PCMPs stored in yogurt (upper) and that of PCMPs after being transported to the GI tract (lower).

Figure 4. Transition after oral administration of FITC-labeled PCMPs in the GI tract of nude mice at different time intervals (from left to right are: the normal group, the control group, the TP5 oral administration group, the TP5 PCMPs yogurt stored 1 day group, and the TP5 PCMPs yogurt stored in 13 days group, respectively).

Figure 5. a-d: Flow cytometry graph of rats in different groups after 7 days of administration (a: control group; b: TP5 oral administration group; c: TP5 injection group; and d: TP5 PCMPs yogurt group); e-h: Flow cytometry graph of immune model rats at different days after administration with the yogurt containing TP5-loaded PCMPs (e: 0 day; f: 2 days; g: 8 days; and h: 16 days).

Figure 6. a-b: CD4/CD8 ratios of rats after continuous administration of TP5-loaded PCMPs with different TP5 dosages for 7 days, with TP5-loaded PCMPs stored in yogurt for 1 day (a) and 19 days (b). And c-d: IgG concentrations in rats after continuous administration of TP5-loaded PCMPs with different TP5 dosages for 7 days, with TP5 PCMPs stored in yogurt for 1 day (c) and 19 days (d). (Low dosage group: 4 mg/kg/d oral administration; medium dosage group: 8 mg/kg/d oral administration; high dosage group: 12 mg/kg/d oral administration).

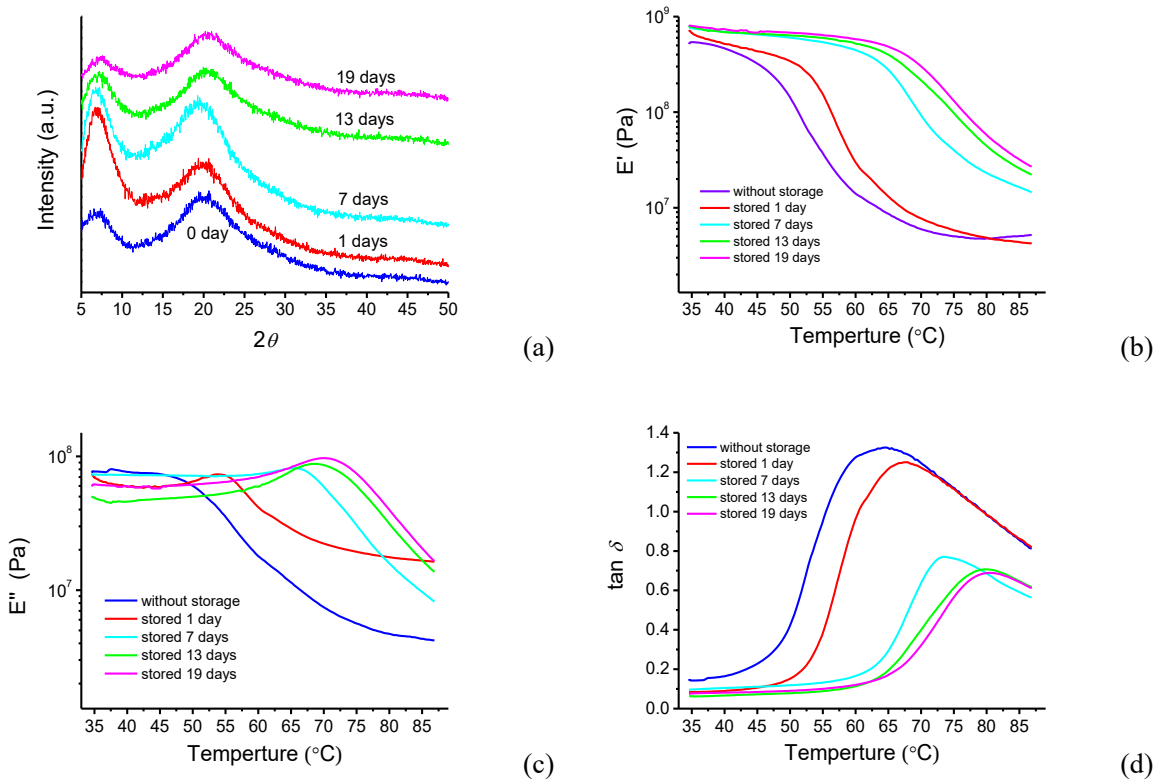
Intensity (a.u.)
19 days
13 days
7 days
0 day
1 days
2θ
(a)
E' (Pa)
without storage
stored 1 day
stored 7 days
stored 13 days
stored 19 days
Temperture (°C)
(b)
E'' (Pa)
without storage
stored 1 day
stored 7 days
stored 13 days
stored 19 days
Temperture (°C)
(c)
tan δ
without storage
stored 1 day
stored 7 days
stored 13 days
stored 19 days
Temperture (°C)
(d)

Figure 1

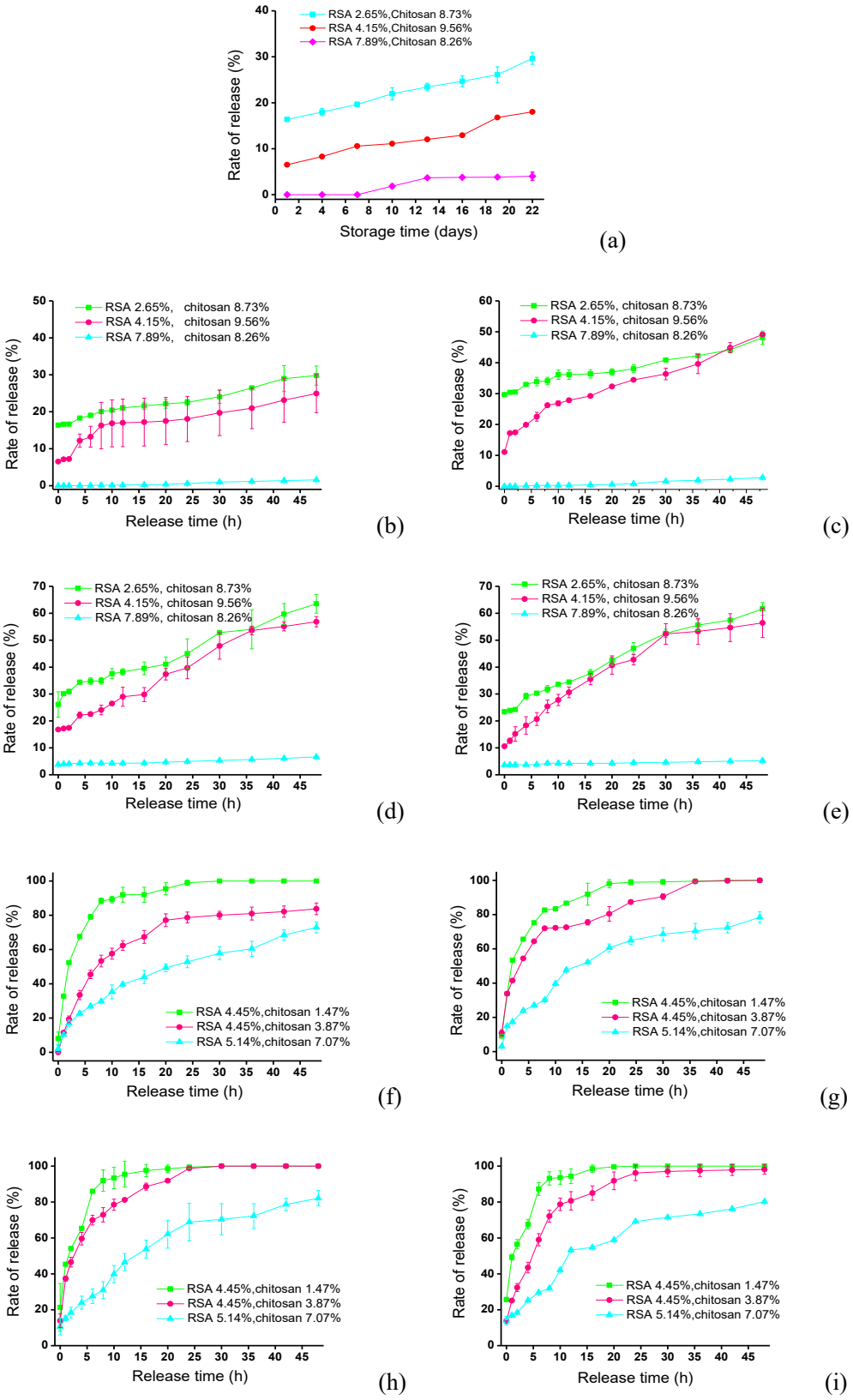
RSA 2.65%,Chitosan 8.73%
RSA 4.15%,Chitosan 9.56%
RSA 7.89%,Chitosan 8.26%
Rate of release (%)
Storage time (days)
(a)
RSA 2.65%, chitosan 8.73%
RSA 4.15%, chitosan 9.56%
RSA 7.89%, chitosan 8.26%
Rate of release (%)
Release time (h)
(b)
(c)
(d)
(e)
RSA 4.45%,chitosan 1.47%
RSA 4.45%,chitosan 3.87%
RSA 5.14%,chitosan 7.07%
(f)
(g)
(h)
(i)

Figure 2

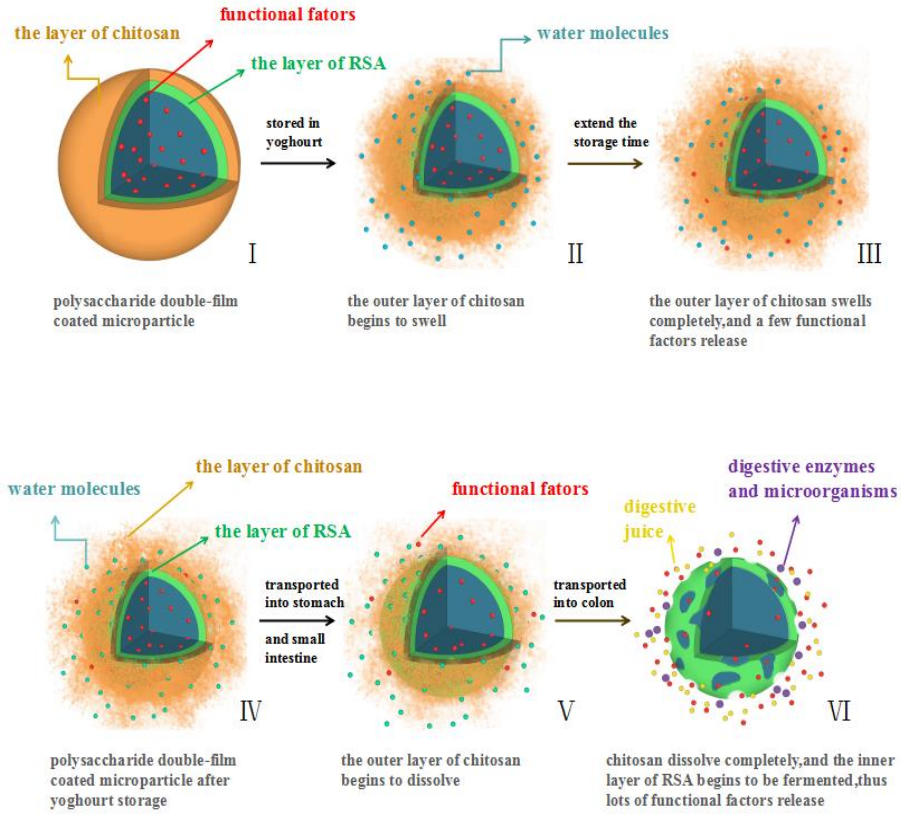
functional fators
the layer of chitosan
the layer of RSA
water molecules
stored in
yoghourt
extend the
storage time
I
II
III
polysaccharide double-film
coated microparticle
the outer layer of chitosan
begins to swell
the outer layer of chitosan swells
completely,and a few functional
factors release
the layer of chitosan
water molecules
functional fators
digestive enzymes
and microorganisms
digestive
juice
the layer of RSA
transported
into stomach
and small
intestine
transported
into colon
IV
V
VI
polysaccharide double-film
coated microparticle after
yoghourt storage
the outer layer of chitosan
begins to dissolve
chitosan dissolve completely,and the inner
layer of RSA begins to be fermented,thus
lots of functional factors release

Figure 3

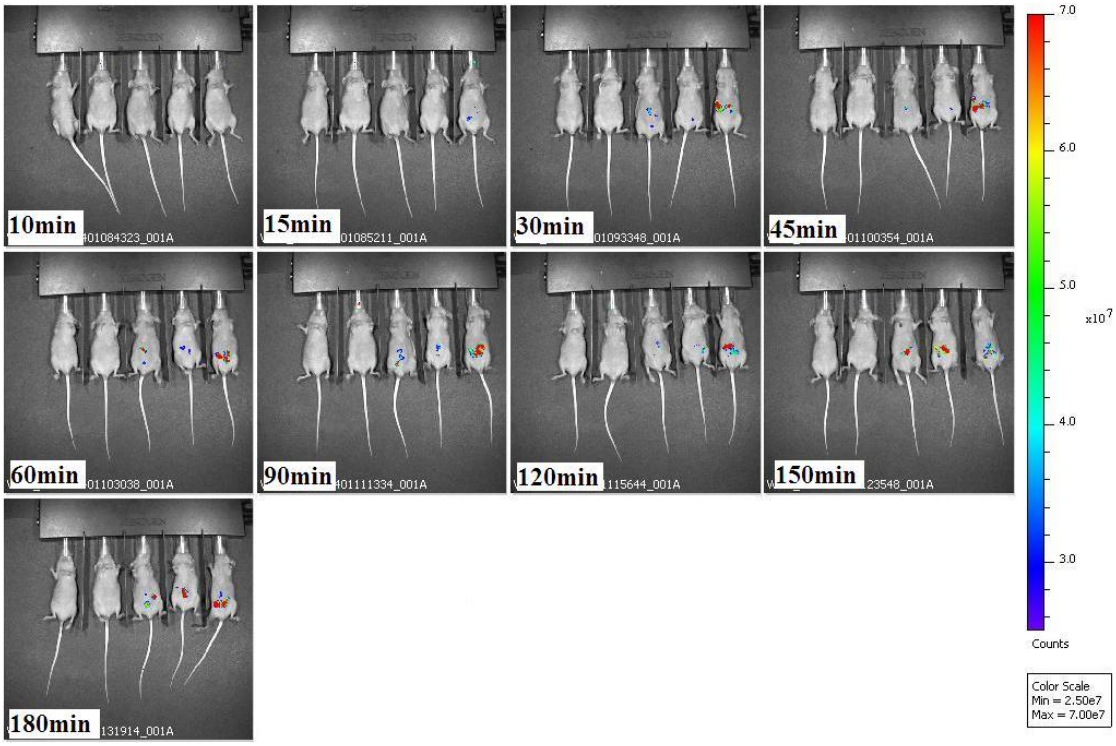
10min
15min
30min
45min
60min
90min
120min
150min
180min
7.0
6.0
5.0
x10^7
4.0
3.0
Counts
Color Scale
Min = 2.50e7
Max = 7.00e7

Figure 4

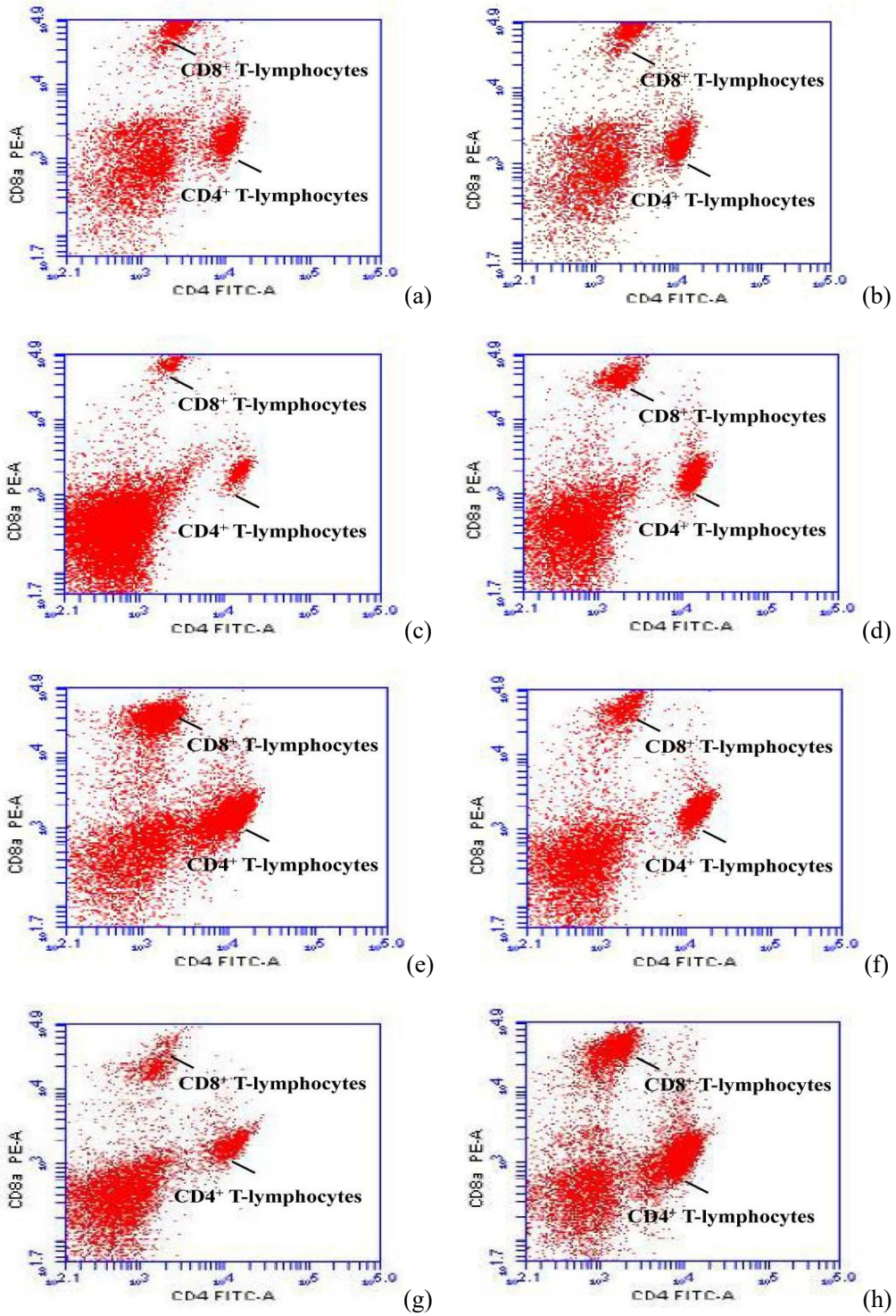
CD8⁺ T-lymphocytes
CD4⁺ T-lymphocytes
CD8a PE-A
CD4 FITC-A
(a)
(b)
(c)
(d)
(e)
(f)
(g)
(h)

Figure 5

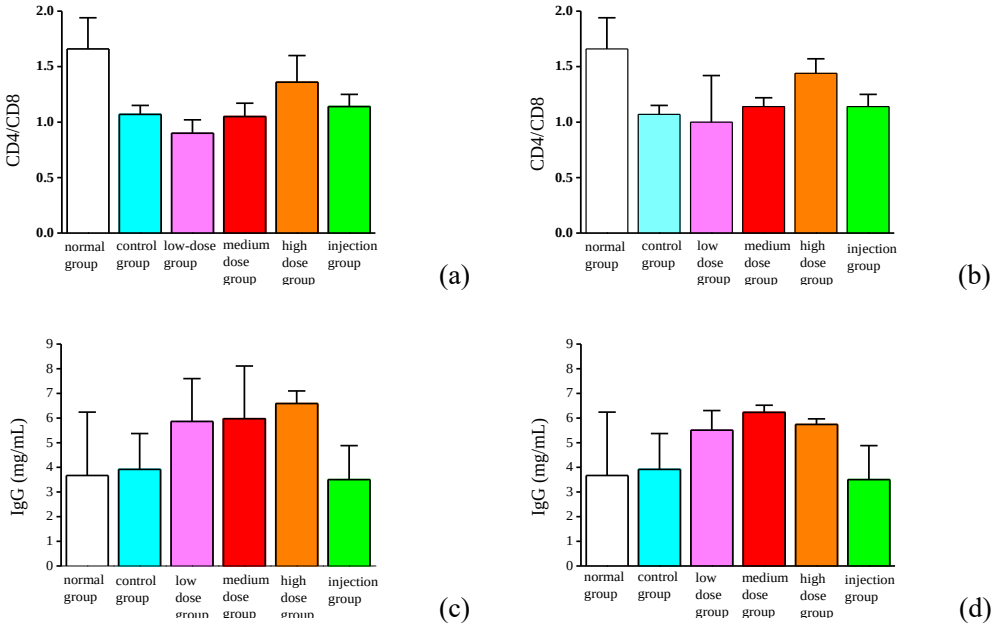
CD4/CD8
2.0
1.5
1.0
0.5
0.0
normal group
control group
low-dose group
medium dose group
high dose group
injection group
(a)
CD4/CD8
2.0
1.5
1.0
0.5
0.0
normal group
control group
low dose group
medium dose group
high dose group
injection group
(b)
IgG (mg/mL)
9
8
7
6
5
4
3
2
1
0
normal group
control group
low dose group
medium dose group
high dose group
injection group
(c)
IgG (mg/mL)
9
8
7
6
5
4
3
2
1
0
normal group
control group
low dose group
medium dose group
high dose group
injection group
(d)

Figure 6

Table 1 Release behaviors of RSA film-coated microparticles and PCMPs (mean±SD)

Release time		0 h	2 h	8 h	24 h	48 h
Stored for 1 day	RSA 4.15%	1.50±2.13	22.78±4.65	39.08±4.32	67.43±2.54	91.54±0.29
	RSA 4.15% + chitosan 9.56%	6.52±0.04	7.22±0.03	16.26±6.29	18.06±6.11	24.92±5.16
	RSA 5.14% + chitosan 7.07%	2.09±2.40	16.94±2.13	29.78±1.01	52.82±3.45	72.90±3.15
Stored for 7 days	RSA 4.15%	5.73±3.44	22.85±0.35	39.80±0.23	64.56±2.40	86.98±4.96
	RSA 4.15% + chitosan 9.56%	11.10±0.01	17.43±0.13	26.23±0.65	34.44±0.05	49.13±0.26
	RSA 5.14% + chitosan 7.07%	3.06±0.40	17.41±0.13	30.14±1.01	64.90±2.45	78.47±3.15
Stored for 13 days	RSA 4.15%	16.39±2.24	36.97±0.24	54.32±0.77	80.14±2.16	100.00±0.00
	RSA 4.15% + chitosan 9.56%	10.58±0.01	15.19±2.67	25.39±2.38	42.76±1.96	56.42±5.45
	RSA 5.14% + chitosan 7.07%	10.66±4.72	18.43±2.93	30.91±4.75	68.82±10.47	82.11±4.29
Stored for 19 days	RSA 4.15%	15.48±5.90	34.22±0.63	50.74±0.25	75.50±0.44	96.12±5.49
	RSA 4.15% + chitosan 9.56%	16.80±0.01	17.43±0.13	24.08±1.79	39.71±1.04	56.85±1.90
	RSA 5.14% + chitosan 7.07%	13.99±2.36	18.47±0.39	31.94±0.42	69.21±0.12	80.23±0.77

Table 2 The ratio of CD4/CD8 and IgG concentrations of rats in different days after administration

Time	Normal group		Control group		TP5 oral administration group		TP5 injection group		TP5 PCMPs yogurt group	
	CD4/CD8	IgG	CD4/CD8	IgG	CD4/CD8	IgG	CD4/CD8	IgG	CD4/CD8	IgG
0d	1.60 ± 0.06^{Aa}	9.82 ± 1.42^{Ab}	1.09 ± 0.25^{Ba}	12.00 ± 0.98^{Ab}	0.90 ± 0.09^{Ba}	12.33 ± 2.32^{Ac}	1.06 ± 0.25^{Ba}	11.81 ± 2.39^{Ab}	0.90 ± 0.17^{Bb}	9.50 ± 1.07^{Ac}
2d	1.53 ± 0.14^{Aa}	11.92 ± 2.77^{Aab}	1.18 ± 0.13^{ABa}	11.90 ± 0.25^{Ab}	0.96 ± 0.11^{Ba}	12.39 ± 1.60^{Ac}	1.19 ± 0.22^{Aba}	12.21 ± 0.60^{Ab}	1.19 ± 0.23^{ABa}	12.15 ± 2.14^{Ab}
5d	1.61 ± 0.29^{Aa}	14.23 ± 0.70^{Aa}	1.14 ± 0.01^{ABa}	14.72 ± 0.51^{Aa}	0.98 ± 0.20^{Ba}	14.09 ± 0.81^{Abc}	1.16 ± 0.14^{Aba}	14.76 ± 1.98^{Aab}	1.33 ± 0.29^{ABab}	15.64 ± 1.16^{Aab}
8d	1.52 ± 0.12^{Aa}	11.22 ± 1.21^{Bab}	1.15 ± 0.11^{Ba}	11.60 ± 1.07^{Bb}	1.11 ± 0.17^{Ba}	16.55 ± 0.94^{Aa}	1.07 ± 0.13^{Ba}	12.95 ± 1.36^{Bb}	1.52 ± 0.16^{Aa}	16.48 ± 1.16^{Aa}
12d	1.52 ± 0.09^{Aa}	14.43 ± 0.31^{Ca}	0.98 ± 0.12^{Ba}	16.44 ± 0.14^{Ba}	0.99 ± 0.06^{Ba}	16.23 ± 1.19^{ABab}	1.03 ± 0.15^{Ba}	13.38 ± 0.52^{Ba}	1.14 ± 0.04^{Bab}	18.71 ± 0.20^{Aa}
16d	1.59 ± 0.15^{Aa}	11.26 ± 0.19^{Aab}	0.82 ± 0.21^{Ba}	15.18 ± 1.23^{Aa}	0.66 ± 0.37^{Ba}	10.92 ± 2.26^{Ac}	0.46 ± 0.08^{Bb}	11.98 ± 1.19^{Ab}	0.89 ± 0.04^{Bb}	10.89 ± 1.92^{Ac}

Values followed by different upper case letters within a column differ significantly ($P < 0.01$); ccapital letters differed from each group at the same time; lower-case letters differed from the time at the same group.